

Adaptive Divergence in Experimental Populations of *Pseudomonas fluorescens*. I. Genetic and Phenotypic Bases of Wrinkly Spreader Fitness

Andrew J. Spiers, Sophie G. Kahn, John Bohannon, Michael Travisano¹ and Paul B. Rainey²

Department of Plant Sciences, University of Oxford, Oxford OX1 3RB, United Kingdom

Manuscript received October 3, 2001

Accepted for publication January 24, 2002

ABSTRACT

A central feature of all adaptive radiations is morphological divergence, but the phenotypic innovations that are responsible are rarely known. When selected in a spatially structured environment, populations of the bacterium *Pseudomonas fluorescens* rapidly diverge. Among the divergent morphs is a mutant type termed “wrinkly spreader” (WS) that colonizes a new niche through the formation of self-supporting biofilms. Loci contributing to the primary phenotypic innovation were sought by screening a WS transposon library for niche-defective (WS⁻) mutants. Detailed analysis of one group of mutants revealed an operon of 10 genes encoding enzymes necessary to produce a cellulose-like polymer (CLP). WS genotypes overproduce CLP and overproduction of the polymer is necessary for the distinctive morphology of WS colonies; it is also required for biofilm formation and to maximize fitness in spatially structured microcosms, but overproduction of CLP alone is not sufficient to cause WS. A working model predicts that modification of cell cycle control of CLP production is an important determinant of the phenotypic innovation. Analysis of >30 kb of DNA encoding traits required for expression of the WS phenotype, including a regulatory locus, has not revealed the mutational causes, indicating a complex genotype-phenotype map.

THE evolution of phenotypic and ecological diversity within a rapidly multiplying lineage (adaptive radiation) is a striking feature of evolution (DARWIN 1859; LACK 1947; DOBZHANSKY 1951; SIMPSON 1953; SCHLUTER 2000). Successive adaptive radiations have generated the majority of ecological diversity on earth and have shaped the morphologies and physiologies of organisms to fit a multitude of environments. The central feature of all adaptive radiations is phenotypic divergence caused by divergent natural selection favoring certain phenotypic innovations that lead lineages along divergent evolutionary trajectories. The nature of these innovations, how they arise and why they are favored by selection, is poorly understood (SCHLUTER 2000).

Insight into the ecological and genetic causes of phenotypic divergence requires knowledge of the moment-by-moment workings of adaptive evolution, but this poses a considerable challenge. It is difficult enough to understand the genetic and physiological causes of an extant phenotype without also explaining the causes of its past and future evolution. One route to progress is to use simple experimental populations that are amenable to both genetic analysis and rigorous ecological experimentation (MORTLOCK 1982; LENSKI *et al.* 1998; RAINEY *et al.* 2000).

Previously we described a model adaptive radiation that occurs when the plant-colonizing bacterium, *Pseudomonas fluorescens*, is propagated in a spatially structured microcosm (a static glass vial containing a nutrient broth medium). When introduced into this environment the ancestral genotype rapidly diversifies, producing a range of morphologically distinct niche specialist genotypes that are maintained by negative frequency-dependent selection. Competition among niche specialists drives the radiation and phenotypic divergence is dependent upon ecological opportunity (RAINEY and TRAVISANO 1998).

Among the extensive array of newly evolved phenotypes is a diverse class of morphs known collectively as “wrinkly spreader” (WS). WS morphs produce distinctive undulate colonies on agar plates and colonize the air-broth interface of spatially structured microcosms. Here we report the result of work that aims to provide a precise and mechanistic account of the evolution of WS (and ultimately all phenotypes) during the course of the *P. fluorescens* radiation. We identify the genes that cause and contribute to the evolutionary success of WS, and we describe the phenotypic target of selection and unravel the relationship between the WS phenotype, niche specialization, and fitness.

MATERIALS AND METHODS

Bacterial strains, growth conditions, and manipulation: The ancestral (wild-type) “smooth” (SM) strain is *P. fluorescens* SBW25 that was isolated from the leaf of a sugar beet plant grown at the University Farm, Wytham, Oxford, in 1989

¹Present address: Department of Biology, University of Houston, Houston, TX 77204.

²Corresponding author: Department of Plant Sciences, University of Oxford, South Parks Rd., Oxford OX1 3RB, United Kingdom. E-mail: paul.rainey@plants.ox.ac.uk

(RAINEY and BAILEY 1996). The ancestral strain was placed at -80° immediately after isolation to minimize lab adaptation. The niche-specialist WS genotype (PR1200) was derived from the ancestral genotype following 3 days of selection in a spatially structured microcosm. PR1253 (SBW25 panB::mini-Tn5-*xyIE*) is a pantothenate-requiring auxotroph of SM and contains mini-Tn5-km-*xyIE* inserted within the first gene (*panB*) of the pantothenate biosynthetic operon (RAINEY 1999). This strain is auxotrophic for pantothenate (a useful marker in competition experiments) and the mutation is neutral in a pantothenate replete environment (see RESULTS). PR1252 (SBW25 Δ *panB*) is also a pantothenate-requiring auxotroph, but differs from PR1253 in that the entire *panB* gene has been deleted (RAINEY 1999).

P. fluorescens strains were cultured at 28° in Luria-Bertani (LB; MILLER 1972), Pseudomonas agar F (PAF; Difco), or King's medium B (KB; KING *et al.* 1954). *Escherichia coli* DH5 α , XLI-Blue MRF' (Stratagene, La Jolla, CA), and S17-1 λ_{pir} (SIMON *et al.* 1983) were cultured at 37° in LB. Antibiotics were used at the following concentrations: ampicillin $100 \mu\text{g ml}^{-1}$, kanamycin $75 \mu\text{g ml}^{-1}$ ($50 \mu\text{g ml}^{-1}$ for *E. coli*), and tetracycline $25 \mu\text{g ml}^{-1}$. Pantothenate was added to media at a final concentration of 0.24% (w/v) where required. CFC (Oxoid) was added to media to select for *P. fluorescens* strains following conjugation. Congo Red was used at a final concentration of 0.001% (w/v) in KB or LB agar without NaCl (NaCl causes Congo Red to precipitate). Calcofluor [Sigma (St. Louis) Fluorescent Brightener 28] was used in LB at $1-10 \mu\text{M}$ and cells or the polymer incubated with the stain for 30 min before examination by fluorescent microscopy.

Cosmid and plasmid DNA were introduced into *E. coli* and *P. fluorescens* by transformation (electroporation) or conjugation using standard procedures. The helper plasmid, pRK2013 (DITTA *et al.* 1980), was used to facilitate transfer of cosmids and plasmids between *E. coli* and *P. fluorescens*.

Molecular biology techniques: Genomic DNA was isolated from *P. fluorescens* using the CTAB procedure (AUSUBEL *et al.* 1990). Plasmid DNA was isolated from *E. coli* using QIAprep plasmid kits (QIAGEN, Chatsworth, CA). DNA was prepared for pulsed-field gel electrophoresis (PFGE) as described previously (RAINEY and BAILEY 1996). PGFE was performed using 1.2% agarose gels in $0.5 \times$ TBE at 200 V with 1- to 25-sec switch times for 22 hr. Standard agarose gel electrophoresis and other recombinant DNA techniques were performed according to SAMBROOK *et al.* (1989). DNA fragments were recovered from agarose using a QIAEX II gel extraction kit (QIAGEN). DNA probes for Southern analysis were labeled and detected using Amersham (Buckinghamshire, UK) enhanced chemiluminescence kits. pSK⁺ (pBluescriptII SK⁺; Stratagene) was used for cloning. The neomycin phosphotransferase plus promoter was derived from plasmid pCPP2988 (ALFANO *et al.* 1996). Allelic exchange was performed using the suicide reporter plasmid pUIC3 (RAINEY 1999). Cellulase (Sigma) was diluted in 50 mM sodium acetate (pH 5.0) buffer at 37° .

DNA sequencing and analysis: DNA sequencing was carried out on an ABI310 (Perkin-Elmer, Norwalk, CT) automated sequencer. Sequence flanking mini-Tn5-km was obtained using primers to the left- and right-hand ends of the transposon (O-end, 5'-ACTTGTGTATAAGAGTCAG; I-end, 5'-TCTAGC GAGGGCTTTACT). Sequence of the *wss* operon was obtained from pSK⁺ clones by a combination of primer walking and direct sequencing of subcloned fragments. Details of the primers and plasmids used for sequencing are available on request. Nucleotide and derived amino acid sequence homology searches were analyzed using the GCG sequence analysis software package. DNA and amino acid homology searches were performed using the National Center for Biotechnology Information BLAST.

Mutagenesis of WS: Transposon mutagenesis was performed using mini-Tn5-km carried by the suicide plasmid pUTkm (HERRERO *et al.* 1990) and was introduced into WS (and SM) by conjugation (SIMON *et al.* 1983). Transconjugants were selected on PAF agar containing CFC and kanamycin, and colonies were screened for loss (or, in the case of mutagenized SM, for gain) of the WS morphology.

Phenotypic characterization of WS⁻ mutants: WS⁻ (mini-Tn5-km) mutants were screened in spatially structured (static broth) microcosms to check for defects in ability to colonize the air-broth interface. Approximately 10^6 cells of each mutant were inoculated into KB broth microcosms (RAINEY and TRAVISANO 1998) and cultures were propagated for 48 hr without shaking. The presence or absence of a mat (biofilm) of cells at the air-broth interface was determined by visual inspection.

To determine the patterns of evolutionary diversification arising from WS⁻ mutants, each mutant was inoculated (in triplicate) into static KB broth microcosms and allowed to evolve for 7 days. Cells were harvested from microcosms by whirli-mixing and the phenotypes of colonies were determined by plating on KB agar. Plates were incubated for 48 hr before recording colony phenotypes.

Fitness of genotypes: Competitive fitness of WS⁻ mutants was determined by directed competition between each mutant and WS (PR1200) in spatially structured microcosms using both kanamycin resistance and smooth colony morphology of WS⁻ mutants to distinguish them from the kanamycin-sensitive WS genotype. Competitive fitness of SM *nptII-wss* was determined by direct competition between SM *nptII-wss* and both SM and WS in spatially structured and unstructured microcosms. The *panB* deletion strain PR1252 was used as the competing ancestral SM genotype and this marker allowed it to be readily distinguished from SM *nptII-wss* and WS. Both PR1252 and SM *nptII-wss* were distinguished from WS on the basis of colony morphology [SM *nptII-wss* also carries a kanamycin (neomycin) resistance maker encoded by *npt*]. Relative fitness was calculated as the ratio of the Malthusian parameters of the two strains being compared (LENSKI *et al.* 1991). Cultures were founded with 10^5 cells of each competitor and the ratio of competing genotypes was determined after 24 hr growth by plating on media containing appropriate antibiotics. All cultures were whirli-mixed for 60 sec before dilution plating in order to maximally disperse clumped cells. (Preliminary experiments showed that after 60 sec of mixing WS cell numbers do not appreciably increase, but WS cells can never be fully dispersed by mixing and therefore WS fitness is always underestimated.)

To determine the importance of the *wss* locus during the course of adaptive radiation, a strain carrying a defective *wss* locus (SM-13) was competed with the pantothenate-marked ancestral SM strain PR1253 in KB broth microcosms supplemented with pantothenate and kanamycin. Cultures were inoculated with $\sim 10^5$ cells of each genotype and microcosms incubated with, or without, shaking for 7 days. The density of each genotype was determined at the start and end of the experiment by plating appropriately diluted aliquots of cells onto KB. PR1253 was distinguished from the derived genotypes by use of the pantothenate marker and marker carriage was confirmed by spraying plates with 1% catechol solution (*xyIE*-expressing cells turn yellow in the presence of catechol). Relative performance of the competing genotypes was quantified using the selection rate constant (the difference in Malthusian parameters of the two competitors; LENSKI *et al.* 1991; TRAVISANO *et al.* 1995). The selection rate constant was used in preference to relative fitness in this experiment because it avoids the problem of dividing by zero, which arises whenever the final density of cells is less than the initial density.

RESULTS

Finding the genes that determine the WS phenotype:

To identify genes responsible for colonization of the air-broth interface we exploited the known correlation between undulate colony morphology on agar plate culture and colonization of the air-broth interface in spatially structured microcosms. Transposon mini-Tn5-km was introduced into the genome of WS and transconjugants were screened for loss of the wrinkled colony morphology. From a screen of 8000 kanamycin-resistant mutants, 40 (WS⁻) mutants with colony phenotypes similar to the ancestral SM genotype were isolated. Subsequent phenotypic checks and elimination of siblings by Southern hybridization reduced the number of unique mutants to 27. With the exception of 2 of these (WS-5 and WS-39), all were defective in their ability to colonize the air-broth interface and behaved like the ancestral genotype. WS-5 and WS-39 formed a very weak mat, but grew primarily in the broth phase.

To verify that colonization of the air-broth interface was the primary cause of enhanced WS fitness (in spatially structured microcosms) all WS⁻ mutants were competed against the “wild-type” WS genotype. A fully balanced competition was not possible because of lack of a neutral marker in WS and carriage of the transposon by the WS⁻ mutants. Nevertheless, over the course of 24 hr all WS⁻ mutants suffered an average reduction in fitness of between 34 and 52%, which is considerably greater than the 3% reduction in fitness attributed to carriage of mini-Tn5-km.

Our ability to produce WS⁻ mutants by transposon mutagenesis suggested that the original mutation causing WS was a gain-of-function mutation. No WS phenotypes were detected following mini-Tn5-km mutagenesis of the ancestral SM genotype.

Phenotypic and genetic characterization of WS⁻ mutants: *Colony morphology:* The colony morphology of each mutant was examined on KB and LB agar after 24, 48, and 72 hr growth. The majority of WS⁻ mutants resembled the ancestral SM strain, which remained smooth irrespective of incubation time or environment. However, the colony phenotypes of mutants WS-6, WS-9, WS-12, WS-18, WS-36, and WS-39 showed plasticity. With the exception of WS-12 and WS-36, colonies formed by these mutants were initially smooth and indistinguishable from the ancestral type, but became gradually more WS-like after 48 hr. WS-12 and WS-36 produced WS-like colonies on LB agar, but produced SM-like colonies on KB. These plastic phenotypes bred true and showed the same patterns of differentiation when cultures were transferred to fresh media. Further examination of the nutrient-dependent expression of WS morphology in WS-12 and WS-36 showed that it was attributable to one or more components of proteose peptone and not due to the repression of this phenotype by a component of KB. WS-5 produced smooth, but slow-growing colonies on both KB and LB.

Cellular morphology: With the exception of WS-39, all WS⁻ mutants (and SM and WS controls) were motile, rod shaped, and indistinguishable from each other by light microscopy, scanning electron microscopy, or transmission electron microscopy (KAHN 1998). WS-39 cells were spherical.

Phenotypic diversification of WS⁻ mutants in static microcosms: To determine the importance of the loci identified by mini-Tn5-km mutagenesis in evolution of WS morphs during selection in a spatially structured microcosm, each of the WS⁻ mutants was inoculated into triplicate microcosms (supplemented with kanamycin to select for the transposon) and incubated without shaking. Patterns of diversity that evolved from each mutant were examined after 7 days of selection by plating onto KB agar supplemented with kanamycin.

Control SM populations diversified to produce a wide range of WS morphs (the dominant class), variant SM types, fuzzy spreader types, and other minor classes as previously described (RAINEY and TRAVISANO 1998). Mutants WS-4, WS-7, WS-11, WS-16, WS-29, and WS-40 generated patterns of diversity that were indistinguishable from the control, suggesting that mutations in these loci were readily compensated for by mutations elsewhere in the genome. A second group of 14 mutants (WS-1, WS-2, WS-13, WS-15, WS-20, WS-21, WS-22, WS-25, WS-27, WS-28, WS-30, WS-33, WS-34, and WS-35) underwent morphological diversification, but failed to generate WS morphs, while a third group of 7 mutants (WS-5, WS-6, WS-9, WS-12, WS-18, WS-36, and WS-39) did not diversify. Taken together, these phenotypic tests enabled the mutants to be subdivided into six different groups (Table 1), with most being assigned to Group II (14 mutants).

Physical mapping of WS⁻ mutants: Southern hybridization was used to determine the genomic distribution of candidate loci identified by mini-Tn5-km insertions. Genomic DNA from each WS⁻ mutant was digested with *ApaI*, *ClaI*, and *KpnI* (which do not cut within mini-Tn5-km) and with *SalI* and *SphI* (which have restriction sites within the transposon) and hybridized to a DNA probe derived from mini-Tn5-km. The majority of transposon insertions were located within three large fragments: an 18.5-kb *KpnI* fragment (5 mutants), a 15.8-kb *ClaI* fragment (14 mutants), or an 8.6-kb *ClaI* fragment (3 mutants). These groupings corresponded closely to the previously identified phenotypic groups (Tables 1 and 2).

To determine whether the three groups of loci were clustered, *SpeI*-digested genomic DNA from representative mutants was hybridized with a DNA probe derived from mini-Tn5-km. The genomic location of each *SpeI* fragment was then checked against the existing physical map (RAINEY and BAILEY 1996). Mutants from Groups I and V were located on *SpeI* fragment SpA, Groups II and III were located on SpH 1, and Group IV was located on SpT. None of these fragments lie adjacent to any

TABLE 1
Classification and phenotypic characterization of WS⁻ mutants

Group	No. in group ^a	Colony morphology ^b	Microcosm diversification ^c			Colonization of air-broth interface ^d
			SM	WS	FS	
I	6	SM	SM	WS	FS	—
II	14	SM	SM	—	FS	—
III	3	SM [†]	SM	—	—	—
IV	2	SM ^{††}	SM	—	—	—
V	1	SM	SM	—	—	±
VI	1	SM [†]	SM	—	—	±

^a Number of unique mutants in group: Group I, WS-4, -7, -11, -16, -29, and -40; Group II, WS-1, -2, -13, -15, -20, -21, -22, -25, -27, -28, -30, -33, -34, and -35; Group III, WS-6, -9, and -18; Group IV, WS-12 and -36; Group V, WS-39; Group VI, WS-5.

^b Colony morphology on KB agar: SM, smooth colonies; SM[†], develops WS-like characteristics after long incubations on KB agar; SM^{††}, SM on KB but WS-like on LB agar; WS, wrinkly spreader-like colonies.

^c Colony morphs that arise after selection (7 days) in spatially structured microcosms; FS, fuzzy spreader-like colonies; —, none detected.

^d Evidence of niche specialization as determined by mat formation in spatially structured microcosms; —, no mat, all growth within the broth phase; ±, thin, easily collapsed mat, most growth in broth phase.

other; no mapping information was obtained for Group VI mutants.

Identity of disrupted loci: Genomic DNA from each transposon mutant was digested with *ApaI*, *Clal*, or *KpnI* and cloned into pSK⁺. Clones containing the transposon and flanking DNA were selected by plating on media supplemented with kanamycin. A total of eight transposon-carrying clones were obtained and the flanking DNA was sequenced from each using primers to either end of the transposon.

Sequence from a single Group I mutant, WS-4, revealed

an open reading frame (ORF; the entire 1002-nucleotide ORF was sequenced; GenBank accession no. AY074937) that was 37% identical at the amino acid level to PleD, a GGDEF-type response regulator from *Caulobacter crescentus*, which in conjunction with PleC and DivK couples polar differentiation and cell cycle processes (HECHT and NEWTON 1995; JENAL 2000). The WS-4 ORF also showed 33% identity to CelR2, which is a putative regulator of cellulose biosynthesis in *Rhizobium leguminosarum* (AUSMEES *et al.* 1999) and 34% identity to AdrA, which is a regulator of cellulose and thin aggre-

TABLE 2
Characterization of WS⁻ mutants by physical mapping and sequence analysis

Group	Mutant	<i>SpeI</i> RF ^a	Linking RF ^b	Gene	Proposed function	Complementation by pCSA/B ^c	Congo Red ^d
I	WS-4	A	18.5 <i>KpnI</i>	<i>wspR</i>	Response regulator	—	—
II	WS-1	H1	15.8 <i>Clal</i>	<i>wssA</i>	Spatial localization	+	—
	WS-13	H1	15.8 <i>Clal</i>	<i>wssB</i>	Cellulose synthase subunit	+	—
	WS-22	H1	15.8 <i>Clal</i>	<i>wssC</i>	Cellulose synthase subunit	+	—
	WS-15	H1	15.8 <i>Clal</i>	<i>wssD</i>	Endoglucanase (cellulase)	+	—
	WS-25	H1	15.8 <i>Clal</i>	<i>wssE</i>	Cellulose synthase subunit	+	—
III	WS-18	H1	8.6 <i>Clal</i>	<i>wssF</i>	Unknown function	+	+
	WS-6	H1	8.6 <i>Clal</i>	<i>wssH</i>	Polymer modification	+	+
	WS-9	H1	8.6 <i>Clal</i>	<i>wssH</i>	Polymer modification	+	+
IV	WS-12	T	7.4 <i>KpnI</i>	<i>pgiA</i>	Phosphoglucose isomerase	—	±
V	WS-39	A	9.4 <i>KpnI</i>	<i>mreB</i>	Murien biosynthesis	—	+
VI	WS-5	ND	13.6 <i>Clal</i> ^e	ND	ND	—	+

ND, not determined.

^a Identity of *SpeI* restriction fragment containing the transposon (see RAINEY and BAILEY 1996).

^b Smallest *ApaI*, *Clal*, or *KpnI* linking fragment (size, in kilobases, includes 2.2 kb of mini-Tn5-km). *SaII* and *SphI* digests were also used to determine the number of unique mutants/replicate mutants within each group.

^c Complementation of genetic lesion by cosmids pCSA and pCSB: —, not complemented; +, complemented.

^d Scored after growth of colonies on KB or LB agar supplemented with Congo Red: —, no uptake of dye; +, uptake of dye; ±, uptake of dye on LB, but not KB agar.

^e Southern analysis indicates that WS-5 is not linked to any other mutants.

gative fimbriae in *E. coli* and *Salmonella typhimurium* (ROMLING *et al.* 2000; ZOGAJ *et al.* 2001). Further *in silico* analysis showed the predicted protein to be comprised of two clearly defined domains separated by a short linker. The N-terminal domain is typical of response regulators and has a conserved aspartate at residue 67 that is the predicted site of phosphorylation. The C-terminal domain is widespread in bacteria, but has no known function. However, recent *in silico* analyses predict that the conserved GGDEF motif is an active site for nucleotide cyclization or hydrolysis (PEI and GRISHIN 2001). Given a probable regulatory function we named this gene *wspR* (WS phenotype regulator). Subsequent sequence analysis has shown that *wspR* is the terminal gene in an operon of seven genes that shows substantial similarity to the “*frz*-like” chemosensory signal transduction pathway of *P. aeruginosa* (STOVER *et al.* 2000; E. BANTINAKI and P. B. RAINEY, unpublished data).

The transposon and flanking DNA were cloned from five Group II mutants. In each instance the DNA sequence showed significant similarity to the *yhj* locus from *E. coli* (SOFIA *et al.* 1994), recently shown to be required for cellulose biosynthesis (ZOGAJ *et al.* 2001), and to genes from *Acetobacter xylinum*, also required for the biosynthesis of cellulose (WONG *et al.* 1990; SAXENA *et al.* 1994). The possibility that this locus encoded the primary structural determinant of the WS morphology led us to name this locus the WS structural locus, *wss* (see below).

No transposons were cloned from Group III mutants, but the three insertions were subsequently mapped by PCR and DNA sequence analysis and shown to be contiguous with the locus identified by the Group II mutants (see below).

The transposon from WS-12, a Group IV mutant, was located in a gene that showed 52% identity to phosphoglucose isomerase (*pgi*) from *Haemophilus influenzae* (FLEISCHMANN *et al.* 1995). PGI is a highly conserved enzyme responsible for the interconversion of glucose-6-phosphate and fructose-6-phosphate.

DNA flanking the transposon in WS-39 (Group V) encodes a putative protein that is 62% identical to MreB from *E. coli*. The *mre* locus in *E. coli* is involved in cell shape determination and progression to cell division (DOI *et al.* 1988; WACHI and MATSUHASHI 1989). No sequence information was obtained for any Group VI mutants.

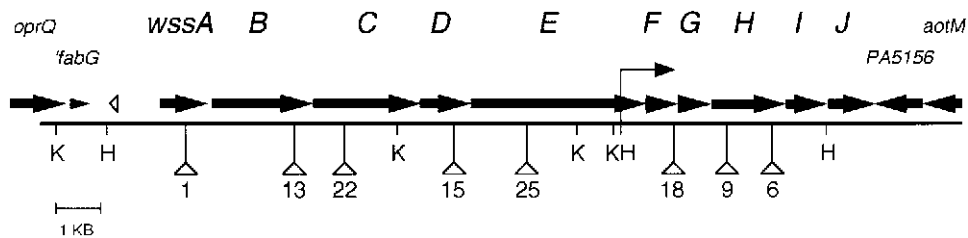
The *wss* locus: *Complementation of Group II and III mutants:* The similarity of the *wss* locus to genes involved in cellulose biosynthesis and the phenotypic data that showed Group II mutants incapable of generating compensatory mutations led us to postulate that this was the primary determinant of the WS phenotype and the innovation responsible for initiating phenotypic divergence. We therefore carried out a detailed analysis of this locus. In the absence of a genome sequence, cosmid clones flanking the region were obtained by screening an existing cosmid library made from wild-type (ances-

tral SM) genomic DNA (RAINEY 1999) with DNA probes derived from the *wss* locus. Two cosmids (pCSA and pCSB) that were shown by restriction analysis to overlap by ~25 kb were obtained. Both cosmids contained restriction fragments that matched the predicted fragment sizes for the disrupted loci of all Group II mutants; both cosmids were able to restore the WS morphology to all Group II mutants. Interestingly, both cosmids were also able to complement the three Group III mutants, suggesting that the locus disrupted in these mutants was closely linked to the *wss* locus. Group I, IV, V, and VI mutants were not complemented by either cosmid.

*The *wss* operon:* The DNA sequence of the central region of cosmid pCSA was obtained from a series of overlapping subclones. Analysis of the nucleotide sequence using FramePlot (ISHIKAWA and HOTTA 1999), which identifies ORFs on the basis of the G + C bias at the third codon position, revealed the presence of 10 ORFs. These ORFs were designated *wssA-J* and form a putative operon (Figure 1). A combination of PCR and sequencing, using primers to both the I- and O-ends of the transposon and to specific sequences within the *wss* operon, allowed all transposons from Group II and III mutants to be mapped to the *wss* operon (Figure 1). A 20-kb nucleotide sequence is available from the GenBank database under accession no. AY074776.

Overall, the *wss* operon shows strong similarity to cellulose biosynthetic clusters from *A. xylinum* and *E. coli* although there are notable differences, particularly at the downstream end (Figure 2). Upstream of the *wss* operon (Figure 1) is a single precursor tRNA encoding tRNA^{Thr} (Cove score = 94.51; LOWE and EDDY 1997), a truncated ORF encoding the C-terminal two-thirds of an oxidoreductase, and a gene showing 77% identity at the amino acid level to outer membrane protein porin Q (*oprQ*) from *P. aeruginosa* (OKAMOTO *et al.* 1999). The truncated ORF shows greatest similarity at the amino acid level (between 36 and 38% identity) to FabG from a wide range of eubacteria. Downstream from *wssJ* the operon is flanked by genes showing strong similarity to an arginine and ornithine transport operon (*aot*; NISHIJYO *et al.* 1998) and a second, closely homologous putative transport operon found in *P. aeruginosa* (STOVER *et al.* 2000). The gene immediately adjacent to *wssJ* encodes a protein that is 68% identical to the hypothetical protein PA5156 of unknown function, and the gene upstream of this is 65% identical to PA5155 and 47% identical to the membrane protein component AotM. Between *wssJ* and *aotM* is an ~1-kb stretch of AT-rich DNA sequence that contains no obvious repeat motifs or terminator structures.

The *wss* operon consists of 10 ORFs (*wssA-J*). The predicted product of *wssA* is a protein of 344 amino acids. It shows greatest similarity to YhjQ from *E. coli* (Table 3), but is also between 23 and 27% identical to MinD from a range of bacteria including *Helicobacter pylori* (27%) and *Bacillus subtilis* (29%). MinD is an



basic cellulose polymer. WssA and WssJ have homology with MinD. Upstream of the *wss* operon is *tRNA^{Thr}* (open arrow), a truncated gene (*'fabG*) encoding an oxidoreductase and a gene predicted to encode a membrane protein porin Q (*oprQ*). Downstream of the operon is a putative arginine and ornithine transport gene (*aotM*) and a hypothetical protein of no known function. The locations of Group II and III mini-Tn5-km transposon insertions are indicated; the position of the *wssE-lacZ* fusion is shown by a rightward facing arrow; H, *HindIII*; K, *KpnI*.

FIGURE 1.—Genetic structure of the *wss* operon. The *wss* operon is a cluster of 10 genes predicted to encode a CLP. The cellulose synthase is predicted to be composed of WssB, WssC, and WssE; WssD is an associated cellulase; WssG, WssH, and WssI are predicted to play a role in acetylation of the

ATPase, which in concert with MinC is responsible for determining cell polarity and the positioning of the septum by FtsZ during cell division (SULLIVAN and MADDOCK 2000). In common with other ATPases of this class, WssA also contains a clearly defined Walker Box. Mutant WS-1 contains a transposon insertion in *wssA* that abolishes the WS phenotype and cellulose production (see below), indicating that this gene, although with no previously recognized role in cellulose biosynthesis (ZOGAJ *et al.* 2001), is part of the *wss* operon.

WssB, WssC, and WssE are predicted to encode proteins of 739, 689, and 1279 amino acids, respectively. Each shows similarity to proteins from *A. xylinum* (Table 3) that together form a cellulose synthase complex (SAXENA *et al.* 1994). Significant similarity also exists at the amino acid level to genes of the *yhj* locus of *E. coli* (BLATTNER *et al.* 1997; Figure 2 and Table 3), recently shown to be involved in cellulose biosynthesis (ZOGAJ *et al.* 2001). On the basis of biochemical analyses of the cellulose synthase complex in *A. xylinum* (SAXENA *et al.* 1994) and *Agrobacterium tumefaciens* (MATTHYSSE *et al.* 1995) WssB is predicted to be the catalytically active subunit of a membrane-bound β -glucan synthase that

polymerizes UDP-glucose into cellulose. Consistent with this prediction is the presence of eight putative membrane-spanning regions in WssB and conservation of DNA sequence surrounding the conserved aspartate residues (U1-4), including the signature motif QXXRW that is characteristic of repetitive transferases involved in the formation of β -glycosidic linkages (SAXENA *et al.* 1994). Also present are the conserved KAG and QTP motifs that are found in both plant and bacterial cellulose synthases and other glycosyltransferases (STASINOPOULOS *et al.* 1999; Blanton *et al.* 2000). WssC and WssE lack transmembrane helices, but are likely to be membrane associated because they are predicted to be closely associated with the catalytic subunit. The amino acid sequence of each protein was analyzed for the existence of signal peptides using both neural networks and hidden Markov chains (NIELSEN *et al.* 1997). Neither WssB nor WssC showed any evidence of a signal sequence; however, WssE is highly likely to have a signal peptide ($P = 1.00$) and to be secreted.

The deduced product of the *wssD* gene (436 amino acids) is a member of the D-family cellulases (β 1-4 glucosidase; Table 2). In *A. xylinum* (SAXENA *et al.* 1994)

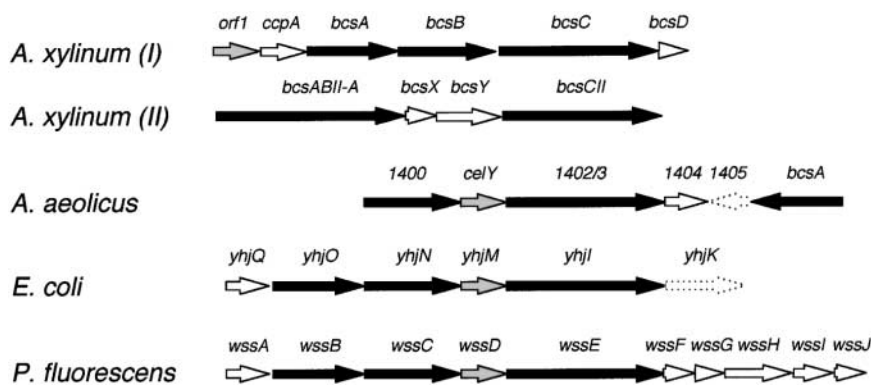


FIGURE 2.—Genetic organization of bacterial cellulose biosynthetic gene clusters. The cellulose biosynthetic operons of *A. xylinum* (*bcsI* and *bcsII*), *Aquifex aeolicus* (putative operon), *E. coli* (*yhj*), and *P. fluorescens* (*wss*) are shown schematically. Each cluster contains the three subunits of the cellulose synthase, although in *bcsII* the first two subunits are fused. Solid arrows, cellulose synthase subunits (*A. xylinum* *bcsAI*, *BI*, and *CI*; *bcsABII-A* and *CII*; *A. aeolicus* *bcsA*, 1400, and 1402/3; *E. coli* *yhjO*, *N*, and *L*; *P. fluorescens* *wssB*, *C*, and *E*). Shaded arrows, cellulase [*A. xylinum* *orf1* (CMCase), *A. aeolicus* *celY*, *E. coli* *yhjM*, and *P. fluorescens* *wssD*]. Open

arrows, genes associated with the cellulose synthase (*A. xylinum* *ccpA* and *bcsX* are of unknown function; *bcsD* is involved in cellulose crystallization; *bcsY* is a putative acetylase; *A. aeolicus* 1404, *E. coli* *yhjQ*, and *P. fluorescens* *wssA* and *wssJ* are *minD* homologs; *P. fluorescens* *wssF* is a homolog of *bcsX*; *wssG*, *wssH*, and *wssI* show similarity to genes encoding proteins involved in acetylation of alginate and are unrelated to *bcsY*). Dotted arrows, genes with no apparent association with cellulose production (*A. aeolicus* 1405 and *E. coli* *yhjK*; WONG *et al.* 1990; RAWLINGS and CRONAN 1992; SAXENA *et al.* 1994; SOFIA *et al.* 1994; STANDAL *et al.* 1994; SAXENA and BROWN 1995; DECKERT *et al.* 1998; OKAMOTO *et al.* 1999).

TABLE 3

Similarity matrix for components of the *wss* operon

<i>P. fluorescens</i>	<i>A. xylinum</i>	<i>E. coli</i>	<i>P. aeruginosa</i>
WssA	—	YhjQ 27/42	—
WssB	BcsA 46/61	YhjO 53/71	—
WssC	BcsB 32/49	YhjN 32/50	—
WssD	CMCase (orf1) 28/44	YhjM 39/53	—
WssE	BcsC 27/40	YhjL 22/36	—
WssF	BcsX 42/54	—	—
WssG	—	—	AlgF 24/38
WssH	—	—	AlgI 43/61
WssI	—	—	AlgJ 32/48
WssJ	—	YhjQ 28/41	—

Similarities between proteins are shown as percentage identical/similar residues. —, no homolog.

and *A. tumefaciens* (MATTHYSSE *et al.* 1995) the cellulase forms an essential part of the cellulose biosynthetic complex. WssF is predicted to encode a protein of 221 amino acids. The amino acid sequence is similar to that encoded by a small ORF (*bcsX*) of unknown function in *A. xylinum* (UMEDA *et al.* 1999; Figure 2).

The genes *wssG*, *wssH*, and *wssI* are predicted to encode proteins of 221, 468, and 374 amino acids, respectively. Homologs of these genes are present in *P. aeruginosa* PAO1 (Table 3) where they are responsible for acetylation of the polysaccharide polymer alginate (FRANKLIN and OHMAN 1996). WssH, like AlgI, has 10 predicted membrane-spanning domains and is likely to be an integral transmembrane protein. WssG possesses a putative signal peptide ($P = 0.976$) and is probably secreted.

The predicted product of the *wssJ* gene is a protein of 324 amino acids. It is similar to WssA at the amino acid level (51% identical), but shows low nucleotide sequence similarity, with only three short stretches of 60–130 nucleotides showing significant (>70%) similarity. Like WssA, WssJ also contains a Walker Box motif.

The wss operon encodes a cellulose-like polymer that provides structural integrity to WS mats: Cellulose is a structurally simple polymer of (1-4)- β -linked linear glucose chains. Given the similarity of several genes of the *wss* operon to those involved in the biosynthesis of cellulose in bacteria and plants, we reasoned that the product of the *wss* operon was cellulose, or at least had a core of (1-4)- β -linked glucose. To test this, the affinity of two dyes, Congo Red and Calcofluor, for WS, SM, and Group II

WS⁻ mutants was determined. Congo Red binds (1-4)- β -D-glucopyranosyl units, basic or neutral extracellular polysaccharides, and some proteins, whereas Calcofluor is a more specific dye for cellulose and binds to (1-3)- β - and (1-4)- β -D-glucopyranosyl units. WS colonies bound Congo Red after 24 hr growth on agar plates containing the dye (the colonies turned bright orange) and, when stained with Calcofluor, copious amounts of filamentous material were observed by fluorescent microscopy. Colonies of the ancestral SM strain showed weak evidence of Congo Red binding and small amounts of Calcofluor-stained material were sometimes observed within cell clumps; however, the Group II WS⁻ mutants bound neither Congo Red nor Calcofluor. In light of this result we hereafter refer to the product of the *wss* operon as “cellulose-like polymer” (CLP).

The Congo Red and Calcofluor binding ability of the remaining WS⁻ mutants were also examined and while all mutants failed to produce wrinkled colonies on agar and colonize the air-broth interface, not all mutants were defective in the production of CLP (Table 2). The most notable exceptions were the Group III strains that contain transposons in the *wss* cluster (*wssG*, *wssH*, and *wssI*), and the *mreB* mutant, WS-39.

Given the overproduction of CLP in the WS genotype (and all other WS genotypes examined) we reasoned that this polymer might be responsible for the structural integrity and rigidity of WS mats. To test this, WS mats were allowed to form by incubation in static broth microcosms; mats were then removed after 3 days and incubated with the enzyme cellulase. Overnight incubation in cellulase caused the WS mats to disintegrate, whereas the integrity of control mats was unaffected (Figure 3).

Transcription of wss in WS and evidence of a regulatory role for WspR: To determine whether CLP overproduction was caused by enhanced transcription of the *wss* locus, the level of *wss* transcription was compared in SM and WS. A chromosomal fusion between *wssE* and the reporter *lacZ* was constructed in both SM and WS by integrating, via homologous recombination, a modified version of an existing *wssE-lacZ* fusion plasmid (GAL 1999) into the chromosomal copy of *wssE* (Figure 1). Correct integration was confirmed by PCR. The level of *wss* expression was determined by monitoring β -galactosidase levels of each fusion strain after growth in LB. A small but significant ($P < 0.01$) increase in the level of *wss* expression was observed in the WS morph at 17 hr; at 29 hr, expression of *wss* in WS was approximately fourfold greater than in SM (Table 4).

An identical *wssE-lacZ* fusion was constructed in the *wspR::mini-Tn 5-km* mutant strain, WS-4, to test the putative regulatory role of WspR in transcription of *wss*. The level of *wss* transcription was also measured after 17 and 29 hr growth in LB (Table 4). In the *wspR*-defective background the level of *wss* transcription reverted to that observed in the ancestral SM genotype, suggesting that WspR plays a regulatory role in *wss* transcription.

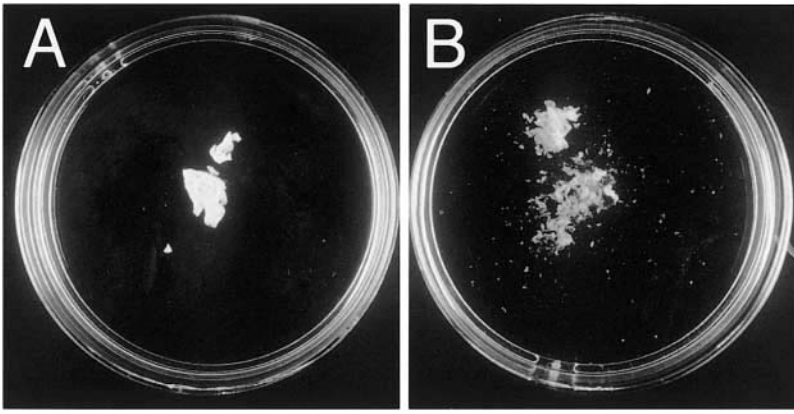


FIGURE 3.—Mat integrity is a result of CLP. Single WS colonies were removed from LB agar plates and incubated in the presence or absence of cellulase. (A) Without cellulase. (B) With cellulase. Colonies were incubated overnight at 37° and then gently agitated before photography.

Elevated transcription of wss does not cause WS: The relatively small (two- to fourfold) difference between transcription of *wss* in SM *vs.* WS suggested that increased transcription of *wss* was not the primary cause of the WS phenotype. To test this hypothesis more rigorously, the level of *wss* transcription was experimentally elevated in the ancestral SM genotype by introducing (by double homologous recombination) the constitutive promoter from the neomycin phosphotransferase gene (*nptII* promoter) 107 nucleotides upstream from the start codon of *wssA*. Enhanced transcription was confirmed by monitoring β -galactosidase levels and CLP production was checked by examining the ability of bacterial strains to bind Congo Red. When grown on agar plates containing Congo Red, the SM *nptII-wss* fusion strain produced bright-orange colonies indicative of CLP production, but did not express the wrinkled colony morphology typical of WS genotypes; growth was primarily in the broth phase and only a weak mat formed at the air-broth interface.

The fact that WS morphology and CLP production were separable traits led to further experiments to determine whether CLP production *per se* was the cause of niche specialization and enhanced ecological performance of WS. To do this, the fitness of SM *nptII-wss* was measured relative to pantothenate-marked ancestral SM (PR1252) and WS in both spatially structured and unstructured microcosms. Overexpression of *wss* slightly

TABLE 4
Transcriptional activity of *wss*

	β -Galactosidase activity	
	17 hr	29 hr
Control	2.6 (0.4)	2.1 (0.6)
SM <i>wssE-lacZ</i>	399 (4.6)	245 (4.9)
WS <i>wssE-lacZ</i>	714 (17.4)	998 (15.2)
WS-4 <i>wssE-lacZ</i>	444 (10)	354 (5.1)

Data are mean Miller Units \pm standard errors from three replicate cultures. WS-4 is *wspR::mini-Tn5-km*.

increased fitness in the spatially structured microcosm, but had no effect in the spatially unstructured microcosm (Table 5). The fitness effects were significantly less beneficial than those measured for the WS genotype; moreover, SM *nptII-wss* did not suffer the marked fitness costs that WS experiences when grown in a spatially unstructured microcosm (Table 5). This result clearly showed that, while necessary, overproduction of CLP alone is not sufficient to generate WS.

Phenotypic divergence, fitness, and the significance of *wss* during adaptive radiation: The results of our molecular-level analysis led to the hypothesis that overproduction of CLP by the *wss* locus is a critical component of the WS adaptive phenotype and a primary cause of the phenotypic innovation upon which selection acts to cause WS to increase in frequency. If true, then an ancestral SM genotype carrying a mutation in the *wss* locus should be competitively inferior, in comparison with the ancestral genotype, during the course of adaptive radiation in the spatially structured microcosms, but not in the spatially unstructured microcosms.

To test this hypothesis a mutation was created in the *wss* locus of the ancestral SM genotype. This was achieved

TABLE 5
Effect of enhanced *wss* transcription on fitness of SM

Spatially	Relative fitness in a spatially structured environment	Relative fitness in an unstructured environment
SM (PR1252)	1.01 (0.02)	0.98 (0.01)
SM <i>nptII-wss</i>	1.10 (0.04)	0.96 (0.02)
WS (PR1200)	1.67 (0.09)	0.33 (0.01)

Data are mean fitness \pm standard errors from three replicate cultures. Relative fitness was measured after 24 hr. Two-way ANOVA test of genotype *vs.* environment for SM and SM *nptII-wss* shows no overall fitness difference between strains ($P = 0.215$), but a slight interaction between genotype and environment (SM *nptII-wss* is slightly fitter than SM in the spatially unstructured environment; $P = 0.054$).

by inserting the mini-Tn5-km transposon into the second gene of the *wss* operon, *wssB*, by allelic replacement, using the transposon and flanking sequence cloned from WS-13 as the source of the recombined DNA. The resulting strain (SM *wssB*::mini-Tn5-km) was named SM-13.

Carriage of mini-Tn5-km by *P. fluorescens* incurs a fitness cost that could potentially be greater than any cost caused by the mutation it generates upon insertion. A valid measure of fitness (SM-13 relative to SM) requires that this cost be taken into account. This was achieved by using strain PR1253 as the competing ancestral SM genotype. PR1253 is a pantothenate auxotroph of SM that carries an insertion of mini-Tn5-km-*xyIE* within the first gene of the pantothenate biosynthetic pathway (*panB*). The mutation itself is neutral in an environment supplemented with pantothenate and cost of carriage of mini-Tn5-km-*xyIE* balances the cost of carriage of mini-Tn5-km by SM-13. PR1253 is readily distinguished from SM-13 on account of auxotrophy and also yellow coloration of colonies after exposure to 1% catechol.

SM-13 (four replicates of three independent SM *wssB*::mini-Tn5-km isolates) was competed directly against PR1253 in both spatially structured and unstructured microcosms. After 7 days of propagation, microcosms were harvested and the population density of the two strains determined. In the spatially unstructured microcosm, SM (PR1253) and SM-13 exhibited equal competitive ability [selection rate constant of SM-13 relative to SM (PR1253): 2.78 ± 3.45 (95% C.I.)] whereas, in the spatially structured microcosm, SM-13 was at a significant fitness disadvantage [selection rate constant of SM-13 relative to SM (PR1253): -5.54 ± 1.93 (95% C.I.)]. No WS morphs were detected in populations derived from SM-13 in either spatially structured or unstructured microcosms.

A notable outcome of competition between SM (PR1253) and SM-13 in spatially structured microcosms was a greater-than-expected fitness deficit in SM-13-derived populations and fewer-than-expected SM-13-derived SM morphs. After 7 days of competition there were approximately two orders of magnitude fewer SM morphs in the SM-13 populations compared with SM morphs derived from SM (PR1253). Our initial expectation was that the fitness of the two evolving populations would be indistinguishable until day 3, when, in the absence of WS morphs from SM-13-derived populations, WS morphs derived from SM (PR1253) would begin to increase in frequency and eventually dominate after 7 days. Given such an outcome, the reduction in fitness of SM-13-derived populations could be directly attributed to the inability of SM-13 to generate WS during the course of the adaptive radiation. However, the smaller-than-expected number of SM-13-derived SM morphs suggests that *wss* is necessary not only for evolution of WS in spatially structured microcosms but also for optimal performance of the ancestral genotype in this envi-

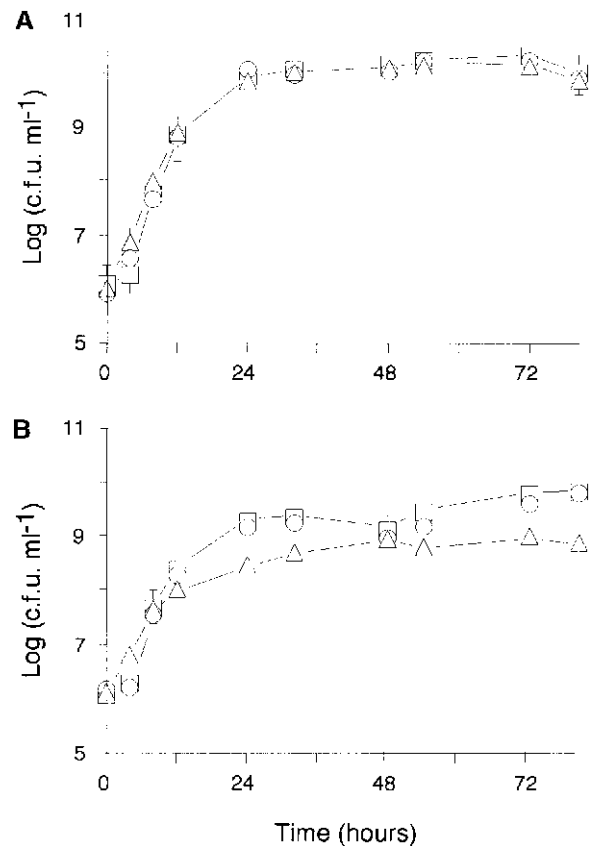


FIGURE 4.—Growth rates of SM, SM-13, and pantothenate-marked SM (PR1253) in spatially unstructured (A) and spatially structured (B) microcosms. Data are means and 95% confidence intervals. Growth rates of all three strains were determined for four replicates at each time point. Circles, SM; triangles, SM-13; squares, SM (PR1253).

ronment. To examine this in more detail, growth curves of SM-13 and SM (PR1253) were determined in both spatially structured and unstructured microcosms during the first 3 days of selection (Figure 4). During this initial period SM morphs are dominant, with evolved WS genotypes being detected only after 48 hr. These data showed that SM-13 had a growth disadvantage relative to SM (PR1253) in spatially structured microcosms, but had no such growth disadvantage over the same period in unstructured microcosms. This indicates that the *wss* operon contributes to fitness of the SM genotype in the spatially structured microcosm and, as a consequence, the fitness loss observed in derived populations of SM-13 can be only partly attributed to the inability of this genotype to generate the WS phenotype during the course of the adaptive radiation.

DISCUSSION

Unravelling the moment-by-moment workings of phenotypic evolution is a challenging task (LEIGH 1999). Here, our efforts to determine the causes of adaptation in a single phenotypic variant of *P. fluorescens* during the

course of adaptive radiation show that even over a short time frame, in a supposedly simple organism, adaptive evolution can be a remarkably complex process.

The top-down (phenotype to genotype) experimental strategy employed here was based upon the conjecture that the genes determining the undulate morphology of WS colonies also determined niche specialization and fitness. The validity of this conjecture was established by showing that transposon mutants of WS that were defective in expression of the wrinkled colony morphology were unable to colonize the air-broth interface of spatially structured microcosms and were competitively inferior to WS. This result demonstrated a direct causal link between the genes that determine colony phenotype and those determining niche specialization and fitness.

Analysis of the niche-defective WS⁻ mutants resulted in their placement into one of six clearly defined groups. A detailed study of the cluster of genes delineated by the Group II mutants was undertaken because it was predicted to encode the primary phenotypic target of selection. A complete sequence analysis of DNA delineated by the Group II mutants revealed a cluster of 10 genes. These genes also complemented loci defined by the phenotypically distinct Group III mutants. The 10 genes are predicted to form a single transcriptional unit (operon) that was designated *wss*. Four of the genes bore significant similarity at the amino acid level to cellulose synthases and cellulases, which in *A. xylinum* (SAXENA *et al.* 1994), *A. tumefaciens* (MATTHYSSE *et al.* 1995), *R. leguminosarum* (AUSMEES *et al.* 1999), and *E. coli* (ZOGAJ *et al.* 2001) are involved in cellulose biosynthesis.

Proof that the *wss* operon encodes a CLP that determines the structural integrity of mats was obtained by applying diagnostic stains to SM, WS, and *wss::mini-Tn5*-km mutants of WS and by treatment of WS mats with the enzyme cellulase. The unique ability of WS to produce CLP and the requirement of this polymer for mat formation and mat integrity gave weight to the hypothesis that this was the cause of niche specialization and the phenotypic innovation primarily responsible for the evolutionary success of WS.

To more rigorously test this hypothesis the evolutionary performance of competing isogenic ancestral SM genotypes—one carrying a nonfunctional *wss* operon and the other wild type—was determined in two contrasting environments. In spatially structured microcosms (the environment within which WS evolved) the population derived from the *wss*-defective ancestor (SM-13) contained no WS morphs and was competitively inferior to the wild type, whereas no significant difference was detected between the competing populations in the spatially unstructured environment. While confirming the importance of the *wss* locus for adaptive evolution of WS and the significance of this phenotype in terms of the overall evolutionary success of the radiating lineage, *wss* was also shown to contribute to the fitness of SM in the spatially structured environment.

It is unclear what role the *wss* operon plays in the ancestral genotype, but given the equivalent ecological performance of SM-13 and SM in the spatially unstructured (shaken) microcosms, clues to biological function and ecological significance of *wss* in the ancestral SM genotype lie in the differences between these two environments. Given that mutations within *wss* are costly during growth in static broth culture, combined with measurable negative pleiotropic effects on growth rate of being WS (P. B. RAINEY, unpublished data), it is interesting that WS mutants are eventually favored by selection during growth in spatially structured microcosms. In this environment a critical point must be reached where the costs of not regulating CLP outweigh the benefits of regulation. A goal of future work is to fully dissect the costs of adaptation associated with the SM-to-WS transition and to map the precise connection between genetic architecture and fitness.

The role of CLP: Several lines of evidence showed that CLP, while necessary for the WS phenotype, niche specialization, and fitness, is not alone sufficient. The first indication came from analysis of the Group III mutants, which despite overproducing the core cellulose polymer, were not WS. The genes defined by the Group III mutants, *wssGHI*, show homology to the *P. aeruginosa* genes *algFIJ*, which together are responsible for acetylation of alginate, a linear exopolysaccharide of D-mannuronate, commonly produced by strains of *P. aeruginosa* (FRANKLIN and OHMAN 1996). It is therefore likely that the cellulose polymer produced by the conserved complex of cellulose synthase enzymes (*wssBCDE*) is also modified in *P. fluorescens*, probably by acetylation. Such a scenario is consistent with the fact that *wssGHI* mutants of WS produce Congo Red staining material, but fail to form undulate colonies or grow at the air-broth interface. Irrespective of the molecular role of *wssGHI*, the products of these genes are essential for full expression of the WS phenotype.

Further proof that CLP production alone does not cause the WS phenotype came from experiments in which the level of transcription of *wss* was experimentally elevated. Ancestral SM containing a *nptII* promoter-fusion to *wss* produced CLP, but failed to express the distinctive wrinkled colony morphology of WS; this genotype was also defective in its ability to colonize the air-broth interface and lacked both the fitness costs and benefits of WS in spatially unstructured and structured microcosms, respectively. The WS phenotype is therefore composed of at least two components—the product of the *wss* operon (CLP) and an additional factor that causes the wrinkled colony morphology.

Several lines of evidence suggest that “wrinkliness” (a marker for the full WS adaptation) might be determined by the localization in time and/or space of CLP production. The first indication of a cell cycle link came from the *mreB* (cell cycle) mutant of WS (WS-39). WS-39 retains the CLP overproducing phenotype of WS but is

unable to express the wrinkled morphology on agar plates or to form a solid WS mat in spatially structured microcosms. The sole difference between WS and WS-39 is the defective murien biosynthetic gene cluster in the latter, which causes cells that are ordinarily rod-shaped to be spherical (JONES *et al.* 2001). A fundamental difference between rod-shaped and spherical cells is the presence of defined cell poles. If CLP production is localized to the poles and the presence of poles is necessary for correct localization of CLP (SHAPIRO and LOSICK 1997), then a cell lacking poles would be expected to display an aberrant phenotype. A further indication that polar localization of CLP might be a significant factor in CLP expression stems from the presence of the two MinD-like (cell cycle) proteins, WssA and WssJ, within the *wss* operon.

The involvement of the putative regulatory protein, WspR, in CLP biosynthesis is also suggestive of a link between cell cycle and CLP production. *In silico* analysis of WspR revealed the protein to be most similar to the cell cycle protein PleD, which is required for polar morphogenesis and correct developmental timing of stalk biogenesis in *C. crescentus* (JENAL 2000). This observation, along with evidence that spatial position of CLP is important, has led to a working hypothesis that postulates that the wrinkly component of the WS phenotype is caused by an alteration in the temporal regulation of CLP. According to this model, in SM, CLP is localized to the cell poles and subject to cell cycle regulation and to regulatory signals transduced through the Wsp chemosensory pathway (E. BANTINAKI and P. B. RAINEY, unpublished results) to WspR. Our prediction is that the WS phenotype is caused by a mutation that alters cell cycle regulation of CLP, causing CLP to be overproduced.

Although a working hypothesis, it provides a simple explanation for the necessity, but insufficiency, of CLP for the WS phenotype. It also accounts for the smooth phenotype of the CLP overproducing strain SM *nptIII-wss* by the fact that correct cell cycle control of CLP (predicted to be exerted at the level of CLP enzyme activity) ought to be intact in this strain. The hypothesis is also supported by recent microscopic analysis of CLP production, which indicates a correlation with the cell cycle in SM (J. BOHANNON, A. J. SPIERS and P. B. RAINEY, unpublished data). Nevertheless, alternative scenarios remain possible and the involvement of as yet unidentified components, such as proteinaceous adhesins, cannot be ruled out.

The genotype to phenotype map: The mutational origins of WS are unknown. Given the speed with which WS morphs arise during the course of selection (within 2 days provided the population size is $>10^8$) and the lack of evidence for an elevated mutation rate to WS (M. TRAVISANO and P. B. RAINEY, unpublished results), it is reasonable to assume that evolution of WS from SM requires just a single mutation. However, given the

substantial amount of heritable variation that exists among independent WS genotypes, it is likely that a variety of different mutations can generate WS. An indication that genetic redundancy exists at a regulatory level is evident by the relative ease with which compensatory mutations arise within the Group I (*wsp*) mutants. This contrasts with the Group II (*wss*) mutants, where no compensatory mutants were detected, suggesting that the *wss* operon is absolutely required for the WS phenotype. Consistent with this prediction is the finding that, from a collection of 50 independently obtained WS genotypes, all overproduced CLP (A. J. SPIERS and P. B. RAINEY, unpublished results).

Each locus identified by mini-Tn 5-km mutagenesis as necessary for the WS phenotype, including the entire *wss* (this study) and *wsp* operons (E. BANTINAKI and P. B. RAINEY, unpublished results), has been sequenced. Comparative sequencing between SM and WS has not yet identified any differences. In addition, genomic DNA from the ancestral SM genotype was shown to complement all *wss* and *wsp* mutants of WS. The mutational causes of WS are therefore likely to lie in regulatory cascades that feed into the *wsp* operon and pass signals onto *wss* (including the *wsp* operon itself). Such an indirect correspondence between the mutational causes of WS and the phenotypic effects engendered is surprising and is a scenario more typical of the complex genotype-phenotype map expected in multicellular eukaryotic organisms.

In bacteria, the mutational causes of adaptive phenotypes have been determined in a small number of instances and, with few exceptions, genotype and phenotype have been shown to be closely linked. Mutations conferring resistance of *E. coli* to antibiotics are typically located in expected targets, for example, *rpsL* (ribosomal protein S12) in the case of streptomycin resistance (SCHRAG *et al.* 1997) and *rpoB* (RNA polymerase) in the case of rifampin resistance (REYNOLDS 2000). TREVES *et al.* (1998) reasoned that acetate cross-feeding mutants of *E. coli* that emerged during selection in glucose-limited chemostats were likely to have elevated levels of acetyl coenzyme A and therefore looked for, and subsequently found, mutations within the promoter region of *acsA* that caused semiconstitutive expression of the enzyme. Similarly, on the basis of *a priori* knowledge of the physiology and genetics of sugar uptake and metabolism in *E. coli*, it was possible to correctly predict mutational targets resulting in improved fitness in glucose during selection in chemostats (NOTLEY-McROBB and FERENCI 1999).

The reason for the complex link between genotype and phenotype in the WS mutants of *P. fluorescens* is unclear, but two factors deserve consideration: the nature of the selective environment and the genetic architecture of *Pseudomonas*. Unlike most other experimental studies of adaptive evolution in bacteria, the *P. fluorescens* radiation occurs in a spatially structured

environment. Adaptation to a new spatially distinct niche is likely to require novel phenotypic innovations, such as those caused by alterations in the timing or location of structural components. Such mutational changes are likely to occur in regulatory cascades that are often physically unlinked to the genes whose effects they control (GERHART and KIRSCHNER 1997).

The prediction that novel phenotypic innovations may stem from mutations in regulatory pathways that control spatial and/or temporal patterns of gene expression comes from studies in developmental genetics (RAFF 1996; CARROLL 2000; STERN 2000). While primarily a concept for understanding the evolution of body plans, there is no reason why this paradigm should not provide an equally valid model for single-celled organisms, which despite their size show considerable developmental complexity (SHAPIRO and LOSICK 1997). Bacteria are not generally multicellular (although see SHAPIRO and DWORKIN 1997) and do not have easily visible surface components; nevertheless, they express a range of proteins, polymers, and macromolecular structures that are often localized on the cell surface and that affect the way individual cells interact with each other and with their environment. Small alterations in the location or timing of expression of these structural components can radically alter the way daughter cells interact with each other and with their environment (GRONEWOLD and KAISER 2001). Our conjecture is that the primary phenotypic innovation responsible for the WS phenotype has arisen through just such a route. Moreover, consistent with our prediction that in bacteria changes in the timing of expression of certain components can have profound effects, we note that evolution of WS from SM involves a transition in the level at which selection acts (MAYNARD SMITH 1988)—from individual SM cells to groups of WS cells. CLP overproduction ensures that daughter cells remain “glued” to one another following cell division and that the combined effect, once magnified through a population, is the formation of a self-supporting mat. In effect, CLP overproduction is part of the mechanism that aligns the interests of individual cells with those of the group, despite the fact that CLP overproduction is costly to the individual WS cell (P. B. RAINEY, unpublished results; a complete analysis of this evolutionary transition will be published elsewhere).

The second factor with possible significance in terms of the evolution of WS is the complexity of the *P. fluorescens* genome. The average *Pseudomonas* genome is ~6.5 Mbp (more than 2 Mbp greater than *E. coli* K12) and is rich in components of signal transduction pathways (STOVER *et al.* 2000), having almost twice the number found in *E. coli* for an equivalent length of DNA (SPIERS *et al.* 2000). These pathways, on account of their modular arrangement, the versatility of individual protein elements, and the weak linkage among components, are thought to confer special properties for the

evolution of phenotypic novelty (GERHART and KIRSCHNER 1997).

Concluding comments: Theory underpinning the ecological causes of adaptive radiation is well developed, but there is no equivalent genetic theory. In light of our understanding of the mechanisms of microevolution it is possible that no such theory is required (LEWONTIN 1974). However, leaving aside debate as to the sufficiency of microevolutionary processes to explain the elaboration of forms in macroevolution (ERWIN 2000), there is growing awareness from studies in evolutionary developmental genetics that certain kinds of mutations are more likely to generate phenotypic novelty than others (SHUBIN *et al.* 1997; STERN 2000). Understanding more precisely what these are, where and when they are likely to occur, and the level at which their effects manifest will be crucial for unravelling the causal connections between variation, selection, and adaptation and for defining the rules of adaptive evolution—should they exist (LEIGH 1999; MORRIS 2000). Clearly, studies with microbial populations can go only so far; but should basic patterns exist, then there is reason to suppose that they will be evident in all forms of life.

We thank E. R. Moxon for early support and encouragement and A. Buckling, R. Kassen, P. Goymier, E. Bantinaki, and two anonymous reviewers for comments on the manuscript. This work was supported by the Biotechnology and Biological Sciences Research Council and the University of Oxford.

LITERATURE CITED

- ALFANO, J. R., D. W. BAUER, T. M. MILOS and A. COLLMER, 1996 Analysis of the role of the *Pseudomonas syringae* pv. *syringae* HrpZ harpin in elicitation of the hypersensitive response in tobacco using functionally non-polar *hrpZ* deletion mutations, truncated HrpZ fragments, and *hrmA* mutations. *Mol. Microbiol.* **19**: 715–728.
- AUSMEES, N., H. JONSSON, S. HOEGLUND, H. LJUNGGREN and M. LINDBERG, 1999 Structural and putative regulatory genes involved in cellulose synthesis in *Rhizobium leguminosarum* bv. *trifolii*. *Microbiology* **145**: 1253–1262.
- AUSUBEL, F. M., R. BRENT, R. E. KINGSTON, D. D. MOORE, J. G. SEIDMAN *et al.*, 1990 *Current Protocols in Molecular Biology*. John Wiley & Sons, New York.
- BLANTON, R. L., D. FULLER, N. IRANFAR, M. J. GRIMSON and W. F. LOOMIS, 2000 The cellulose synthase gene of *Dictyostelium*. *Proc. Natl. Acad. Sci. USA* **97**: 2391–2396.
- BLATTNER, F. R., G. PLUNKETT, A. BLOCH, N. T. PERNA, V. BURLAND *et al.*, 1997 The complete genome sequence of *Escherichia coli* K-12. *Science* **277**: 1453–1474.
- CARROLL, S. B., 2000 Endless forms: the evolution of gene regulation and morphological diversity. *Cell* **101**: 577–580.
- DARWIN, C., 1859 *The Origin of Species*. Muttay, London.
- DECKERT, G., P. V. WARREN, T. GAASTERLAND, W. G. YOUNG, A. L. LENOX *et al.*, 1998 The complete genome of the hyperthermophilic bacterium *Aquifex aeolicus*. *Nature* **392**: 353–358.
- DITTA, G., S. STANDFIELD, D. CORBIN and D. R. HELINSKI, 1980 Broad host range DNAS cloning system for gram-negative bacteria: construction of a gene bank of *Rhizobium melioli*. *Proc. Natl. Acad. Sci. USA* **77**: 7347–7351.
- DOBZHANSKY, T., 1951 *Genetics and the Origin of Species*. Columbia University Press, New York.
- DOI, M., M. WACHI, F. ISHINO, S. TOMIOKA, M. ITO *et al.*, 1988 Determinants of the DNA sequence of the *mreB* gene and of the gene

- products of the *mre* region that function in the formation of the rod shape of *Escherichia coli* cells. *J. Bacteriol.* **170**: 4619–4624.
- ERWIN, D. H., 2000 Macroevolution is more than repeated rounds of microevolution. *Evol. Dev.* **2**: 78–84.
- FLEISCHMANN, R. D., M. D. ADAMS, O. WHITE, R. A. CLAYTON, E. F. KIRKNESS *et al.*, 1995 Whole-genome random sequencing and assembly of *Haemophilus influenzae* Rd. *Science* **269**: 496–512.
- FRANKLIN, M. J., and D. E. OHMAN, 1996 Identification of *algI* and *algJ* in the *Pseudomonas aeruginosa* alginate biosynthetic gene cluster which are required for alginate O acetylation. *J. Bacteriol.* **178**: 2186–2195.
- GAL, M., 1999 Development of “in vivo expression technology” (IVET) and its use to isolate *Pseudomonas fluorescens* genes induced in the plant rhizosphere. D. Phil. Thesis, University of Oxford, Oxford.
- GERHART, J., and M. KIRSCHNER, 1997 *Cells, Embryos, and Evolution*. Blackwell, Malden, MA.
- GRONWOLD, T. M. A., and D. KAISER, 2001 The act operon controls the level and time of C-signal production for *Myxococcus xanthus* development. *Mol. Microbiol.* **41**: 744–756.
- HECHT, G. B., and A. NEWTON, 1995 Identification of a novel response regulator required for the swarmer-to-stalked-cell transition in *Caulobacter crescentus*. *J. Bacteriol.* **177**: 6223–6229.
- HERRERO, M., V. DE LORENZO and K. N. TIMMIS, 1990 Transposon vectors containing non-antibiotic resistance selection markers for cloning and stable chromosomal insertion of foreign genes in gram-negative bacteria. *J. Bacteriol.* **172**: 6557–6567.
- ISHIKAWA, J., and K. HOTTA, 1999 FramePlot: a new implementation of the Frame analysis for predicting protein-coding regions in bacterial DNA with a high G+C content. *FEMS Microbiol. Lett.* **174**: 251–253.
- JENAL, U., 2000 Signal transduction mechanisms in *Caulobacter crescentus* development and cell cycle control. *FEMS Microbiol. Rev.* **24**: 177–191.
- JONES, L. J. F., R. CARBALLIDO-LOPEZ and J. ERRINGTON, 2001 Control of cell shape in bacteria: helical, actin-like filaments in *Bacillus subtilis*. *Cell* **104**: 913–922.
- KAHN, S. G., 1998 Molecular characterisation of genes essential for adaptive evolution in *Pseudomonas fluorescens* SBW25. D. Phil. Thesis, University of Oxford, Oxford.
- KING, E. O., M. K. WARD and D. C. RANEY, 1954 Two simple media for the demonstration of pyocyanin and fluorescin. *J. Lab. Clin. Med.* **44**: 301–307.
- LACK, D., 1947 *Darwin's Finches*. Cambridge University Press, Cambridge, UK.
- LEIGH, E. G., 1999 The modern synthesis: Ronald Fisher and creationism. *Trends Ecol. Evol.* **14**: 495–498.
- LENSKI, R. E., M. R. ROSE, S. C. SIMPSON and S. C. TADLER, 1991 Long-term experimental evolution in *Escherichia coli*. I. Adaptation and divergence during 2,000 generations. *Am. Nat.* **138**: 1315–1341.
- LENSKI, R. E., J. A. MONGOLD, P. D. SNIEGOWSKI, M. TRAVISANO, F. VASI *et al.*, 1998 Evolution of competitive fitness in experimental populations of *E. coli*: What makes one genotype a better competitor than another? *Antonie Leeuwenhoek* **73**: 35–47.
- LEWONTIN, R. C., 1974 *The Genetic Basis of Evolutionary Change*. Columbia University Press, New York.
- LOWE, T. M., and S. R. EDDY, 1997 tRNAscan-SE: a program for improved detection of transfer RNA genes in genomic sequence. *Nucleic Acids Res.* **25**: 955–964.
- MATTHYSSE, A. G., S. WHITE and R. LIGHTFOOT, 1995 Genes required for cellulose synthesis in *Agrobacterium tumefaciens*. *J. Bacteriol.* **177**: 1069–1075.
- MAYNARD SMITH, J., 1988 Evolutionary progress and levels of selection, pp. 219–230 in *Evolutionary Progress*, edited by M. H. NITTECKI. Chicago University Press, Chicago.
- MILLER, J., 1972 *Experiments in Molecular Genetics*. Cold Spring Harbor Laboratory Press, Cold Spring Harbor, NY.
- MORRIS, S. C., 2000 Evolution: bringing molecules into the fold. *Cell* **100**: 1–11.
- MORTLOCK, R. P., 1982 Metabolic acquisitions through laboratory selection. *Annu. Rev. Microbiol.* **36**: 259–284.
- NIELSEN, H., J. ENGELBRECHT, S. BRUNAK and G. VON HEIJNE, 1997 A neural network method for identification of prokaryotic and eukaryotic signal peptides and prediction of their cleavage sites. *Int. J. Neural Sys.* **8**: 581–600.
- NISHIJO, T., S. M. PARK, C. D. LU, Y. ITOH and A. T. ABDELAL, 1998 Molecular characterization and regulation of an operon encoding a system for transport of arginine and ornithine and the ArgR regulatory protein in *Pseudomonas aeruginosa*. *J. Bacteriol.* **180**: 5559–5566.
- NOTLEY-MCROBB, L., and T. FERENCI, 1999 Adaptive *mgl*-regulatory mutations and genetic diversity evolving in glucose-limited *Escherichia coli* populations. *Environ. Microbiol.* **1**: 33–44.
- OKAMOTO, K., N. GOTOH, H. TSUJIMOTO, H. YAMADA, E. YOSHIHARA *et al.*, 1999 Molecular cloning and characterisation of the *oprQ* gene coding for outer membrane protein OprE3 of *Pseudomonas aeruginosa*. *Micobiol. Immunol.* **43**: 297–301.
- PEI, J. M., and N. V. GRISHIN, 2001 GGDEF domain is homologous to adenylyl cyclase. *Proteins* **42**: 210–216.
- RAFF, R. A., 1996 *The Shape of Life: Genes, Development, and the Evolution of Animal Form*. The University of Chicago Press, Chicago.
- RAINEY, P. B., 1999 Adaptation of *Pseudomonas fluorescens* to the plant rhizosphere. *Environ. Microbiol.* **1**: 243–257.
- RAINEY, P. B., and M. J. BAILEY, 1996 Physical map of the *Pseudomonas fluorescens* SBW25 chromosome. *Mol. Microbiol.* **19**: 521–533.
- RAINEY, P. B., and M. TRAVISANO, 1998 Adaptive radiation in a heterogeneous environment. *Nature* **394**: 69–72.
- RAINEY, P. B., A. BUCKLING, R. KASSEN and M. TRAVISANO, 2000 The emergence and maintenance of diversity: insights from experimental bacterial populations. *Trends Ecol. Evol.* **15**: 243–247.
- RAWLINGS, M., and J. E. CRONAN, 1992 The gene encoding *Escherichia coli* acyl carrier protein lies within a cluster of fatty acid biosynthetic genes. *J. Biol. Chem.* **267**: 5751–5754.
- REYNOLDS, M. G., 2000 Compensatory evolution in rifampin-resistant *Escherichia coli*. *Genetics* **156**: 1471–1481.
- ROMLING, U., M. ROHDE, A. OLSEN, S. NORMARK and J. REINKOSTER, 2000 AgfD, the checkpoint of multicellular and aggregative behaviour in *Salmonella typhimurium* regulates at least two independent pathways. *Mol. Microbiol.* **36**: 10–23.
- SAMBROOK, J., E. F. FRITSCH and T. MANIATIS, 1989 *Molecular Cloning: A Laboratory Manual*. Cold Spring Harbor Laboratory Press, Cold Spring Harbor, NY.
- SAXENA, I. M., and R. M. BROWN, 1995 Identification of a second cellulose synthase gene (*ascAII*) in *Acetobacter xylinum*. *J. Bacteriol.* **177**: 5276–5283.
- SAXENA, I. M., K. KUDLICKA, K. OKUDA and R. M. BROWN, 1994 Characterization of genes in the cellulose-synthesizing operon (*acs* operon) of *Acetobacter xylinum*: implications for cellulose crystallization. *J. Bacteriol.* **176**: 5735.
- SCHLUTER, D., 2000 *The Ecology of Adaptive Radiation*. Oxford University Press, Oxford.
- SCHRAG, S. J., V. PERROT and B. R. LEVIN, 1997 Adaptation to the fitness costs of antibiotic resistance in *Escherichia coli*. *Proc. R. Soc. Lond. Biol. Sci.* **264**: 1287–1291.
- SHAPIRO, J. A., and M. DWORKIN (Editors), 1997 *Bacteria as Multicellular Organisms*. Oxford University Press, Oxford.
- SHAPIRO, R. L., and R. LOSICK, 1997 Protein localization and cell fate in bacteria. *Science* **276**: 712–718.
- SHUBIN, N., C. TABIN and S. CARROLL, 1997 Fossils, genes and the evolution of animal limbs. *Nature* **388**: 639–648.
- SIMON, R., U. PRIEFER and A. PUHLER, 1983 A broad host range mobilisation system for *in vivo* genetic engineering: random and site-specific transposon mutagenesis in gram-negative bacteria. *Biotechnology* **1**: 784–791.
- SIMPSON, G. G., 1953 *The Major Features of Evolution*. Columbia University Press, New York.
- SOFIA, H. J., V. BURLAND, D. L. DANIELS, G. PLUNKET, III and F. R. BLATTNER, 1994 Analysis of the *Escherichia coli* genome. V. DNA sequence of the region from 76.0 to 81.5 minutes. *Nucleic Acids Res.* **22**: 2576–2586.
- SPIERS, A. J., A. BUCKLING and P. B. RAINEY, 2000 The causes of *Pseudomonas* diversity. *Microbiology* **146**: 2345–2350.
- STANDAL, R., T. G. IVERSON, D. H. COUCHERON, E. FJÆRVIK, J. M. BLATNY *et al.*, 1994 A new gene required for cellulose production and a gene encoding cellulolytic activity in *Acetobacter xylinum* are co-localised with the *bcs* operon. *J. Bacteriol.* **176**: 665–672.
- STASINOPOULOS, S. J., P. R. FISHER, B. A. STONE and V. A. STANISICH, 1999 Detection of two loci involved in (1-3)- α -glucan (curdlan) biosynthesis by *Agrobacterium* sp. ATCC31749, and comparative sequence analysis of the putative curdlan synthase gene. *Glycobiology* **9**: 31–42.

- STERN, D., 2000 Evolutionary developmental biology and the problem of variation. *Evolution* **54**: 1079–1091.
- STOVER, C. K., X. Q. PHAM, A. L. ERWIN, S. D. MIZOGUCHI, P. WARRENER *et al.*, 2000 Complete genome sequence of *Pseudomonas aeruginosa* PA01, an opportunistic pathogen. *Nature* **406**: 959–964.
- SULLIVAN, S. M., and J. R. MADDOCK, 2000 Bacterial division: finding the dividing line. *Curr. Biol.* **10**: R249–R252.
- TRAVISANO, M., F. VASI and R. E. LENSKI, 1995 Long-term experimental evolution in *Escherichia coli*. III. Variation among replicate populations in correlated responses to novel environments. *Evolution* **49**: 189–200.
- TREVES, D. S., S. MANNING and J. ADAMS, 1998 Repeated evolution of an acetate-crossfeeding polymorphism in long-term populations of *Escherichia coli*. *Mol. Biol. Evol.* **15**: 789–797.
- UMEDA, Y., A. HIRANO, M. ISHIBASHI, H. AKIYAMA, T. ONIZUKA *et al.*, 1999 Cloning of cellulose synthase genes from *Acetobacter xylinum* JCM 7664: implication of a novel set of cellulose synthase genes. *DNA Res.* **6**: 109–115.
- WACHI, M., and M. MATSUHASHI, 1989 Negative control of cell division by *mreB*, a gene that functions in determining the rod shape of *Escherichia coli* cells. *J. Bacteriol.* **171**: 3123–3127.
- WONG, H. C., A. L. FEAR, R. D. CALHOON, G. H. EICHINGER, R. MAYER *et al.*, 1990 Genetic organisation of the cellulose synthase operon in *Acetobacter xylinum*. *Proc. Natl. Acad. Sci. USA* **87**: 8130–8134.
- ZOGAJ, X., M. NIMTZ, M. ROHDE, W. BOKRANZ and U. ROMLING, 2001 The multicellular morphotypes of *Salmonella typhimurium* and *Escherichia coli* produce cellulose as the second component of the extracellular matrix. *Mol. Microbiol.* **39**: 1452–1463.

Communicating editor: H. OCHMAN